Conf-910817--29

WSRC-MS--91-179

DE92 009657

DEVELOPMENT OF J-INTEGRAL BASED UT FLAW ACCEPTANCE CRITERIA FOR SAVANNAH RIVER REACTORS TANKS (U)

by

H. S. Mehta[1], S. Ranganath[1], N. G. Awadalla[2], R. L. Sindelar[2], G. R. Caskey, Jr.[2], and W. L. Daugherty[2]

[1] GE Nuclear Energy
San Jose, California

[2] Westinghouse Savannah River Company
Savannah River Site
Aiken, South Carolina 29808

A paper proposed for presentation at the
SMIRT Conference
Tokyo, Japan

and for publication in the proceedings

This paper was prepared in connection with work done under Contract No. DE-AC09-89SR18035 with the U.S. Department of Energy.

DEVELOPMENT OF J-INTEGRAL BASED UT FLAW ACCEPTANCE CRITERIA FOR SAVANNAH RIVER REACTOR TANKS

H. S. Mehta, S. Ranganath
GE Nuclear Energy, San Jose, Ca USA

N. G. Awadalla, R. L. Sindelar. G. R. Caskey, Jr., W. L. Daugherty
Westinghouse Savannah River Company
Savannah River Laboratory, Aiken, SC USA

1 INTRODUCTION AND BACKGROUND

The tank of a Savannah River Site reactor is a cylinder approximately 16 feet in diameter and 14 feet high and is not pressurized except for a 5 psig helium blanket gas in addition to the hydrostatic head of the heavy water (D_2O) moderator. The tank is made of American Iron and Steel Institute Type 304 Stainless steel fabricated into cylindrical shells with 0.5 inch thick four to six wrought plates per vessel. The shell was made up in two flat half-sections for later rolling and welding. The tank bottom section containing the moderator effluent nozzles was welded to the shell in a T-joint configuration. All joining was performed with multipass Metal Inert Gas (MIG) welding. Figure 1 shows a schematic of the reactor tank.

An ultrasonic (UT) in-service inspection program has been developed for the examination of these reactor tanks. Prior to the initiation of these inspections, criteria for the disposition of any indications that may be found were required. This paper describes the fracture mechanics evaluations that formed the technical bases for the flaw acceptance criteria.

The fracture mechanics evaluation considered detailed finite element calculated stress states in the various regions of the tanks, measured irradiated fracture toughness properties (irradiated condition material J-R curves), fluence levels in the tanks, and intergranular stress corrosion cracking (IGSCC) growth rates in the reactor environment. The irradiation program was conducted at the High Flux Isotope Reactor at Oak Ridge National Laboratory. Tensile and fracture toughness data were obtained from 36 compact tension, tensile and Charpy V-notch specimens.

Through wall cracks are postulated in various regions of the tank and critical crack lengths are calculated by the elastic-plastic fracture mechanics based J-Integral/Tearing Modulus (J/T) approach. The applied values of J-integral were calculated by the well-known GE/EPRI estimation scheme. Acceptable crack lengths are then calculated following generally accepted safety factors based on the ASME Pressure Vessel Code. The acceptance criteria are then briefly described.

2 STRESS AND STRUCTURAL EVALUATION

The major portion of the tank wall is a thin-walled cylinder with no structural discontinuities. The bottom tube sheet assembly is treated as a composite flat plate incorporating the stiffness of numerous piping penetrations as well as the perforated top and bottom plates comprising the bottom shield surfaces. The applied loadings considered were internal pressure, thermal gradient and seismic. Finite element techniques were applied to calculate the stresses used in the fracture mechanics assessment were determined at two postulated through wall crack locations (see Figure 1). Crack A is oriented in the axial direction and crack B is circumferentially oriented. These two locations are the most severe for the given orientation.

The load states considered in the fracture assessment were; (i) normal operations, (ii) normal operation + design basis earthquake (DBE) and (iii) accident condition. The last two load states fall under the faulted or Level D condition defined by the ASME code. For the axial crack (location A) the accident condition stresses are more limiting than the normal operation + DBE case. On the other hand, normal operation + DBE condition \stresses are more limiting for the circumferential crack (location B). The loadings during both the normal and accident conditions are pressure, thermal gradient and the weld residual stress.

Based on a review of the technical literature, a self-equilibrated weld residual stress distribution was assumed. For this distribution, the peak stress magnitude occurs as a tensile stress at both surfaces of the wall, and as a compressive stress at mid-wall. For points in between, linear interpolation is used to get the residual stress. Table 1 summarizes the applied and weld residual stress values used in the fracture mechanics evaluation.

3 MATERIAL TENSILE AND FRACTURE TOUGHNESS PROPERTIES

Irradiations conducted as part of the Reactor Materials Program (RMP) provided mechanical property data for fast fluence (E > 0.1 MeV) and displacement damage levels at or above tank wall fluence levels.

A tensile stress-strain curve was developed based on a review of the stress-strain data from Type 304 stainless steel specimens irradiated to levels comparable to the SRS reactor tank walls. This stress-strain curve was characterized in the Ramberg-Osgood format as follows:

$$\left(\frac{\varepsilon}{\varepsilon_o}\right) = \left(\frac{\sigma}{\sigma_o}\right) + \alpha\left(\frac{\sigma}{\sigma_o}\right)^n$$

with, $\alpha = 4.2$, $n = 8.9$, $\sigma_o = 90000$ psi, $\varepsilon_o = \sigma_o/E$ and $E = 28\mathrm{x}10^6$ psi.

The J-resistance curves used in the evaluation were generated from tests on HFIR-irradiated SRS material. A review of the J-Resistance curve data from all of the specimens irradiated in the HFIR 4M assembly, showed that the specimen 7HAH5 exhibited the lowest toughness. Therefore, the J-Resistance curve data (Figure 2) from this specimen were conservatively used in the fracture mechanics evaluation. The J-integral values in Figure 2 are based on deformation J-integral [1]. Comparable values based on modified J-integral were also calculated, but the more conservative deformation J values were used in establishing the acceptance criteria. Since the J-Resistance curve in Figure 2 appears to go through an inflection point at a J of ≈650 in-lb/in^2, only the data points up to that point were used in determining the material J-T curve based on the data in Figure 2.

Since the expected values of applied tearing modulus (T, app), will be considerably smaller than the lowest tearing modulus values on the J-T curve, a horizontal straight line extrapolation from the highest J value was conservatively used as shown in Figure 3.

4 FRACTURE MECHANICS EVALUATION

The calculation procedure for the postulated axial through-wall crack (location A in Figure 1) is illustrated. The loadings considered for this case are internal pressure, thermal gradient and weld residual stress. Since the stress due to pressure is essentially membrane type, the J-integral values were calculated by the following formulas [2, 3]:

$$\frac{J}{Y^2 \sigma_o \varepsilon_o \alpha} = n\,[1 + \frac{1}{2}\left(\frac{n-1}{n+1}\right)\left(\frac{Y\sigma}{\sigma_o}\right)^2]\left(\frac{\sigma}{\sigma_o}\right)^2$$

$$+ \alpha\,[3.85\sqrt{n}\left(1 - \frac{1}{n}\right) + \frac{\pi}{n}\left(\frac{\sigma}{\sigma_o}\right)$$

$$Y^2 = 1 + 1.25\,\lambda^2 \qquad (0 < \lambda < 1)$$

$$= (0.6 + 0.9\lambda)^2 \qquad (1 < \lambda < 5)$$

$$\lambda = \sqrt{Rt}$$

where,

- a = half crack length
- l = shell parameter
- R = reactor tank radius
- t = reactor tank thickness

a, n, σ_0 ε_0 and E are Ramberg-Osgood parameters defined earlier. The stress due to thermal gradient loading is essentially pure bending. Therefore, standard formulas for calculating K due to a bending stress were used [4].

Due to the self-equilibrated nature of the weld residual stress distribution, standard solutions for stress intensity factors in the literature cannot be directly used to calculate the applied K. Therefore, finite element analyses were used to determine the K values.

A cylinder representing the tank was modeled by two layers of 20 node brick elements. The correct singularity at the crack tip was assured by using isoparametric brick elements with quarter point nodes. The residual stress distribution was applied in the form of nodal loads on the nodes at the crack surface. The peak magnitude of the stress in these analyses was 45 ksi. For the two crack lengths analyzed (2a= 3 and 12 inches), the calculated K values were 21 and 27 ksi$\sqrt{}$ in, respectively.

It is seen that the calculated K values do not follow the conventional dependence of K and $\sqrt{a}$. This is due to the fact that the assumed through thickness residual stress distribution is unusual in the sense that it produces zero net force on the crack face. Based on energy considerations, it is logical to expect that as the through-wall crack lengthens, the stress intensity factor does not continue to increase. The calculated K values are consistent with this. The K values for other crack lengths were obtained by fitting a curve to the calculated values. The curve fit function was selected such that as the crack length increases, the K value asymptotically reaches a constant value.

The combining of J-integral values from various loadings is described next. Based on the fast fluence level, the yield strength of the material at both the locations analyzed is expected to be no greater than 85 ksi. Thus, for the given loadings the material fracture behavior is expected to be in the small scale yielding regime. Therefore, it is reasonable to add the K values from various loadings to obtain a K_{total}. The addition of the individual K values is needed since the J values are nonlinear functions of stress and are not additive. The K_{total} was then converted into an equivalent J_{total} value by the usual relationship, $J=K^2/E$.

The elastic plastic fracture mechanics based concepts developed by Paris and Hutchinson [5, 6] were used to determine the instability crack lengths at both the locations. The applied J-integral (J, app or J_{total}) was calculated as a function of crack length for normal and accident condition loads. The applied tearing modulus (T, app) is defined as: T, app = (E / σ_0^2) [d (J, app) / da]. The intersection of (J, app; T, app) and the (J, mat; T, Mat) curve gives the instability point. From the J, app value at instability, the crack length corresponding to instability can be determined.

Pressure vessels designed to the ASME Code provide, in general, a safety factor of 3 on pressure against failure due to vessel rupture under design conditions. For faulted conditions (or Level D) the code provides a safety factor of 1.41. The same safety factors were used in this evaluation. These safety factors were only applied to the pressure and seismic stresses. This is realistic since the objective is to provide safety factors that provide margins on applied loading.

Table 3 shows a summary of the calculated values of instability and allowable crack lengths. The allowable crack lengths are equal to the instability crack lengths with the pressure and seismic stresses multiplied by appropriate safety factors. The allowable crack lengths at location A are smaller than those at location B. The lowest allowable crack length at location A is 25 inches. This crack length was conservatively used in the development of tank flaw acceptance criteria.

5 IGSCC BEHAVIOR

The austenitic stainless steel of the SRS reactor tanks is susceptible to IGSCC. Laboratory studies of crack growth rate at SRS conditions were conducted under both constant load and slow cyclic load with CT specimens. The observed crack growth rates were of the order of 10^{-6} in/hour under steady state conditions and were between 10^{-5} to 10^{-4} inch/hour under transient conditions. An upper bound crack growth rate of 10^{-4} inch/hour was assumed in developing the acceptance criteria. For a crack growing at both ends, this produces a growth of 1.75 inch/year.

6 ACCEPTANCE CRITERIA

The minimum allowable crack length in Table 2, the IGSCC growth rate and a conservative safety factor based on engineering judgment was used in arriving at reexamination standard and acceptance standard crack lengths as discussed next.

Two standards are defined for characterizing UT indications. With the exception of the geometric reflectors, an indication greater than or equal to 20% through-wall in depth is considered a flaw. Detection of flaws smaller than those used for UT qualification is not required. However, if smaller indications are detected, they would be recorded and considered by the analyst for combination with adjacent indications, if any.

The acceptance standard is 10 inches. A safety factor of 2 was applied to the minimum allowable crack length of 25 inches. From this was subtracted the expected crack growth over an 18 month period. This gives the 10 inch value. Flaws greater than or equal to the acceptance standard require additional analysis and evaluation using flaw, material, and operating conditions specific to the flaw location to determine the continued acceptability. Flaws shorter than the acceptance standard are acceptable for continued operation for a period of 18 months.

The reexamination standard is 5 inches. This value is obtained by applying a safety factor of 2 to the acceptance standard, based on the engineering judgment of SRS Tank Acceptance Criteria Working Group. Flaws which are smaller than the reexamination standard are acceptable for continued operation until the next normal inspection in 5 years.

7 CONCLUSIONS

The technical basis of a fracture mechanics based flaw acceptance criteria for SRS reactor tanks is described. The fracture mechanics analyses show that the SRS reactor tanks can tolerate large cracks while still maintaining Code required safety margins. The criteria can be used to disposition any indications that may be found by in-service UT examination.

ACKNOWLEDGEMENT

The authors gratefully acknowledge the contribution of the following members of the SRS Tank Acceptance Criteria Working Group, in developing the acceptance criteria: D. C. Adamonis, N. P. Baumann, J. A. Begley, S. H. Bush, W. E. Cooper, J. G. Merkle, J. C. Tobin and S. Yukawa. The information contained in this article was developed during the course of work done under Contract No. DE-AC09-765R0000, (now DE-AC09-895R18035) with the U. S. Department of Energy.

REFERENCES

1. Ernst, H. A., "Material Resistance and Instability Beyond J-Controlled Crack Growth, "ASTM STP 803, 1983, pp. 1191-1213.
2. Shih, C. F. and Hutchinson, J. W., "Fully Plastic Solutions and Large Scale Yielding Estimates for Plane Stress Crack Problems, "Trans. of ASME, vol. 98, pp. 289-295 (1976).
3. Paris, P. C. And Tada, H., NUREG/CR-3464, September 1983.
4. D. P. Rooke and D. J. Cartwight, "Compendium of Stress Intensity Factors, "HMS Office, London, September 1974.
5. Paris, P. C., Tada, H., Zahoor, A. and Ernst, H, "The Theory of Instability of the Tearing Mode of Elastic-Plastic Crack growth," ASTM STP 668, pp. 5-36, 1979.
6. Hutchinson, J. W. And Paris, P. C., "Stability Analysis of J-Controlled Crack Growth,"STP ASTM 668, pp. 37-64, 1979.

TABLE 1

STRESS MAGNITUDES AT POSTULATED CRACK LOCATIONS

Location	Load Source	Stress (psi) Membrane	Stress (psi) Bending
A	Pressure, NO	2525	0
	Pressure, Acc.	5228	0
	Th. Gradient, NO	0	3240
	Th. Grad., Acc.	0	6480
B	Pressure, NO	500	1000
	Th. Gradient, NO	0	0
	Seismic (DBE)	5000	0

Note: A self-equilibrated weld residual stress distribution was assumed at both locations. The peak stress magnitude was 30000 psi at location A and 45000 psi at location B.

NO= Normal Operation

TABLE 2

CALCULATED INSTABILITY AND ALLOWABLE CRACK LENGTHS

Postulated Crack Location	Load State	Instability Crack Length (inch)	Allowable Crack Length (inch)
A	NO	58	26
	Acc	32	25
	Acc + DBE	32	25
B	NO	----	----
	No + DBE	50	40
	Acc + DBE	46	36

Notes: NO= Normal Operation
Acc= Accident Condition
DBE= Design Basis Earthquake

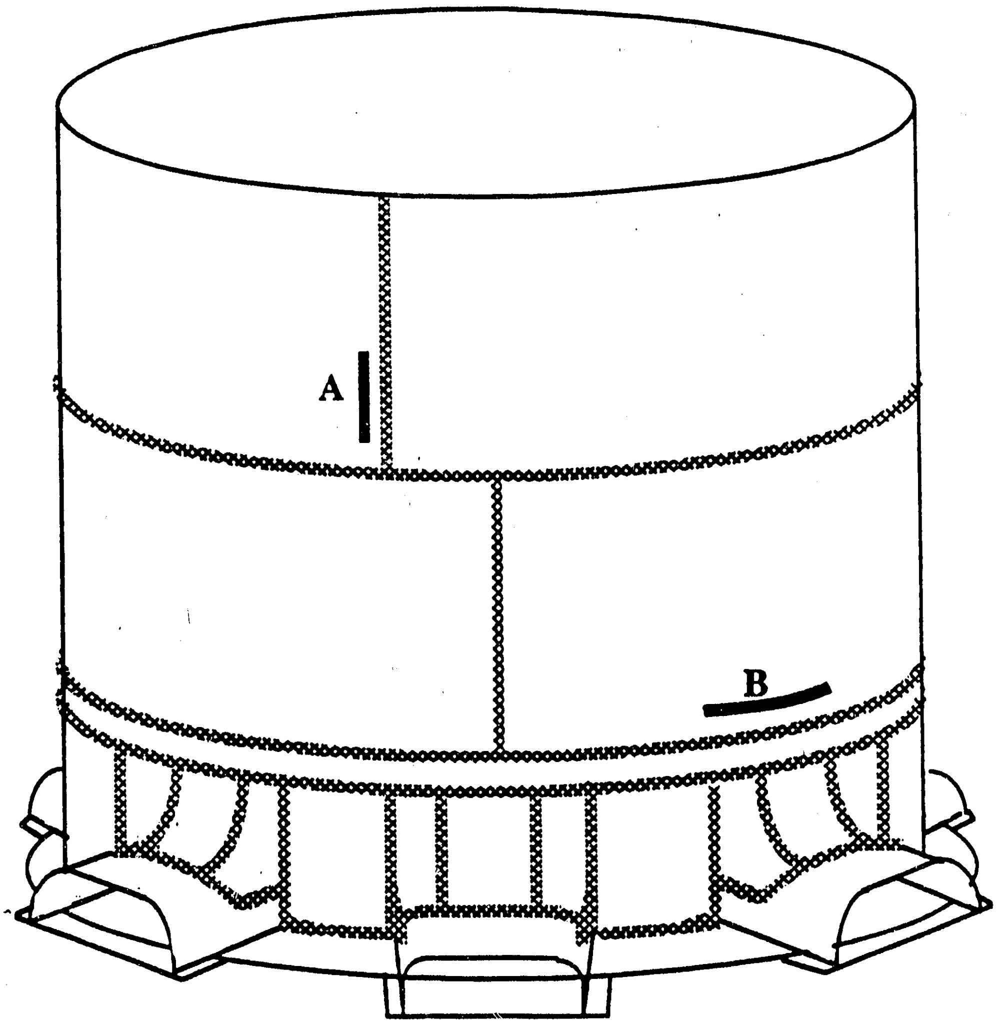

Figure 1. Postulated Crack Locations

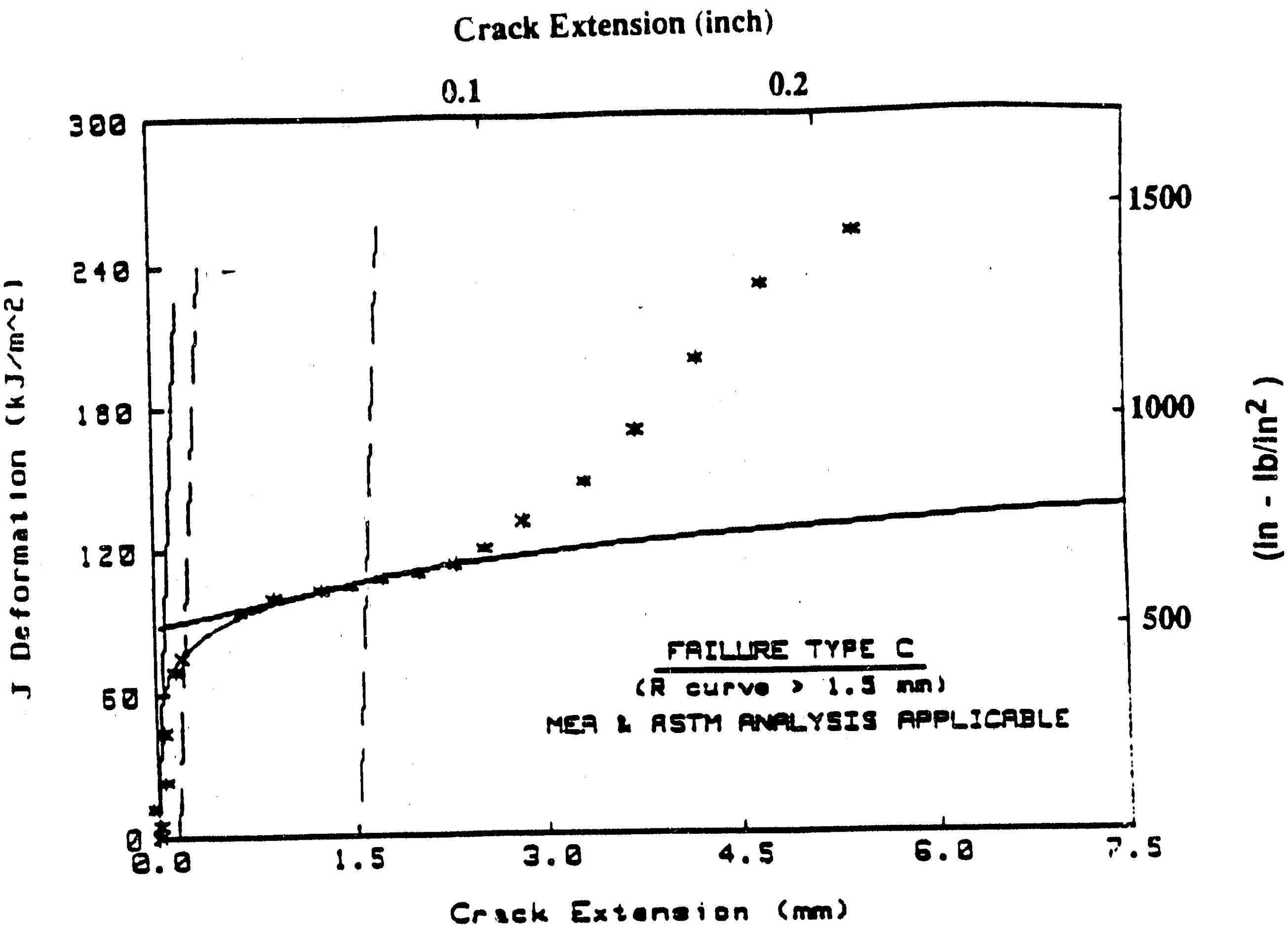

Figure 2: J Deformation curve for specimen 7HAH5

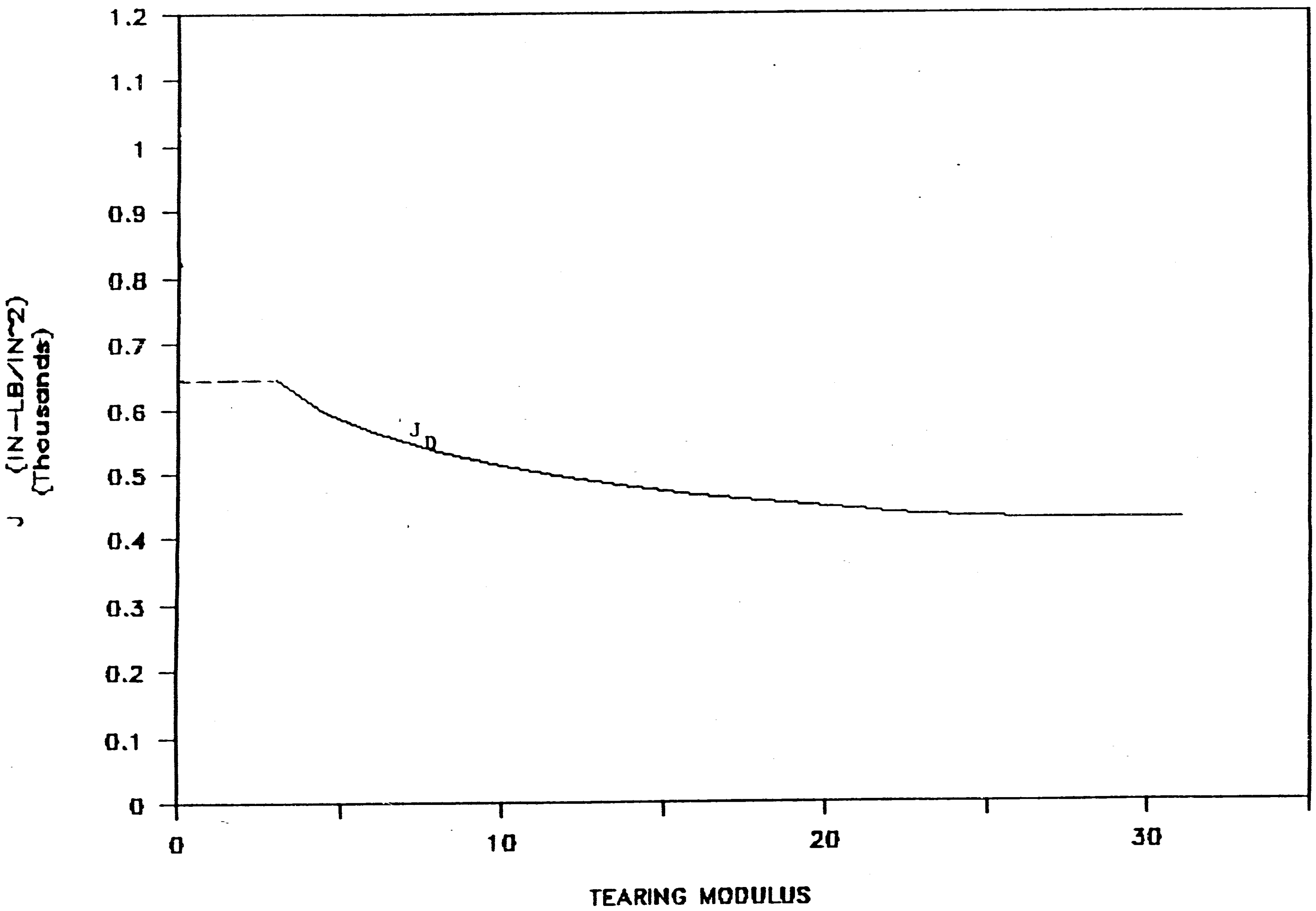

Figure 3. Irradiated material J-T curve based on J Deformation from 7HAH5

END

DATE
FILMED
4/24/92